Received: 8 May 2019 | Revised: 11 November 2019 | Accepted: 3 December 2019

DOI: 10.1096/fj.201901028RR

RESEARCH ARTICLE

THE FASEB JOURNAL

Increased levels of Aβ42 decrease the lifespan of *ob/ob* mice with dysregulation of microglia and astrocytes

Mitsuru Shinohara[1,2] | Yoshitaka Tashiro[1] | Motoko Shinohara[1] | Junko Hirokawa[1] | Kaoru Suzuki[1] | Miyuki Onishi-Takeya[3] | Masahiro Mukouzono[4] | Shuko Takeda[4] | Takashi Saito[5,6] | Akio Fukumori[1,2] | Takaomi C. Saido[5] | Ryuichi Morishita[4] | Naoyuki Sato[1,2]

[1]Department of Aging Neurobiology, Center for Development of Advanced Medicine for Dementia, National Center for Geriatrics and Gerontology, Morioka, Japan

[2]Department of Aging Neurobiology, Graduate School of Medicine, Osaka University, Suita, Japan

[3]Department of Geriatric Medicine, Graduate School of Medicine, Osaka University, Suita, Japan

[4]Department of Clinical Gene Therapy, Graduate School of Medicine, Osaka University, Suita, Japan

[5]Laboratory for Proteolytic Neuroscience, RIKEN Center for Brain Science, Wako, Japan

[6]Department of Neurocognitive Science, Nagoya City University Graduate School of Medical Science, Nagoya, Japan

Correspondence
Naoyuki Sato, Head of the Department of Aging Neurobiology, Center for Development of Advanced Medicine for Dementia, National Center for Geriatrics and Gerontology, 7-430, Morioka, Obu, Aichi 474-8511, Japan.
Email: nsato@ncgg.go.jp

Funding information
This work was supported in part by Research Funding for Longevity Sciences from NCGG (28-45 to NS); Grants-in-Aid from Japan Promotion of Science; the Japanese Ministry of Education, Culture, Sports, Science and Technology (MEXT26293167, MEXT15K15272 & MEXT17H04154 to NS; 17H07419 & 18H02725 to MiS); a Takeda Science Foundation Research Encouragement Grant (to NS and MiS); a SENSHIN Medical Research Foundation Research Grant (to NS); a Novartis Foundation for Gerontological Research Award (to NS);

Abstract

Clinical studies have indicated that obesity and diabetes are associated with Alzheimer's disease (AD) and neurodegeneration. Although the mechanisms underlying these associations remain elusive, the bidirectional interactions between obesity/diabetes and Alzheimer's disease (AD) may be involved in them. Both obesity/diabetes and AD significantly reduce life expectancy. We generated $App^{NL\text{-}F/wt}$ knock-in; *ob/ob* mice by crossing $App^{NL\text{-}F/wt}$ knock-in mice and *ob/ob* mice to investigate whether amyloid-β (Aβ) affects the lifespan of *ob/ob* mice. $App^{NL\text{-}F/wt}$ knock-in; *ob/ob* mice displayed the shortest lifespan compared to wild-type mice, $App^{NL\text{-}F/wt}$ knock-in mice, and *ob/ob* mice. Notably, the Aβ42 levels were increased at minimum levels before deposition in $App^{NL\text{-}F/wt}$ knock-in mice and $App^{NL\text{-}F/wt}$ knock-in; *ob/ob* mice at 18 months of age. No differences in the levels of several neuronal markers were observed between mice at this age. However, we observed increased levels of glial fibrillary acidic protein (GFAP), an astrocyte marker, in $App^{NL\text{-}F/wt}$ knock-in; *ob/ob* mice, while the levels of several microglial markers, including CD11b, TREM2, and DAP12, were decreased in both *ob/ob* mice and $App^{NL\text{-}F/wt}$ knock-in; *ob/ob* mice. The increase in GFAP levels was not observed in young $App^{NL\text{-}F/wt}$ knock-in; *ob/ob* mice.

Abbreviations: Aβ, β-amyloid; AD, Alzheimer's disease; APP, amyloid precursor protein; CNS, central nervous system; DEA, diethylamine; GFAP, glial fibrillary acidic protein; INSR, insulin receptor; IRS1, insulin receptor substrate-1; IRS2, insulin receptor substrate-2; PDK1, pyruvate dehydrogenase kinase 1; PSD95, post-synaptic density protein 95; SYT1, synaptotagmin 1; NF-H, neurofilament heavy chain.

an Annual Research Award Grant from the Japanese Society of Anti-aging Medicine (to NS); a Takeda Medical Research Foundation Research Grant (to NS); a research grant from the Japan Foundation For Aging And Health (to MiS); and a research grant from the Uehara Memorial Foundation (to MiS)

Thus, the increased Aβ42 levels may decrease the lifespan of *ob/ob* mice, which is associated with the dysregulation of microglia and astrocytes in an age-dependent manner. Based on these findings, the imbalance in these neuroinflammatory cells may provide a clue to the mechanisms by which the interaction between obesity/diabetes and early AD reduces life expectancy.

KEYWORDS

Alzheimer's disease, astrocytes, diabetes, lifespan, microglia, obesity

1 | INTRODUCTION

Clinical studies have indicated that obesity and diabetes are associated with Alzheimer's disease (AD) and neurodegeneration,[1,2] although the mechanisms underlying this association remain elusive.[3,4] Both obesity and diabetes are associated with a significant reduction in life expectancy.[5-7] Dementia also shortens the life expectancy; estimates of median survival after the onset of dementia range from 5 to 10 years.[8] However, it has not been clearly determined whether obesity/diabetes and Alzheimer's disease (AD) interact with each other to modulate the lifespan. Moreover, the mechanisms by which diabetes and AD decrease the life expectancy have not been elucidated.

Bidirectional interactions may exist between obesity/diabetes and AD.[3,9] Obesity/diabetes causes neurodegeneration by inducing dysfunction of vascular systems, glucose metabolism, and insulin signaling, as well as by modifying β-amyloid (Aβ)/tau metabolisms.[9-16] In turn, AD influences systemic glucose metabolism by inducing behavioral changes, memory disturbances, hypothalamic dysfunction, frailty, and possibly changes in plasma/peripheral Aβ levels.[9,17-21] Thus, various molecular, cellular, inter-organ, physical, and clinical factors might contribute to the bidirectional interactions between obesity/diabetes and AD.[3]

In the present study, we have investigated whether Aβ affects the lifespan of *ob/ob* mice by crossing $App^{NL\text{-}F/wt}$ knock-in mice and *ob/ob* mice. $App^{NL\text{-}F/wt}$ knock-in; *ob/ob* mice have the shortest lifespan than wild-type mice, $App^{NL\text{-}F/wt}$ knock-in mice, and *ob/ob* mice. Notably, Aβ42 levels were increased before deposition in $App^{NL\text{-}F/wt}$ knock-in mice and $App^{NL\text{-}F/wt}$ knock-in; *ob/ob* mice, but their levels were mostly comparable in these mice. Moreover, both $App^{NL\text{-}F/wt}$ knock-in; *ob/ob* mice and *ob/ob* mice showed decreased levels of microglial markers and only $App^{NL\text{-}F/wt}$ knock-in; *ob/ob* mice showed increased levels of an astrocyte marker. Thus, increased levels of Aβ42 may shorten the lifespan of *ob/ob* mice with dysregulation of microglia and astrocytes.

2 | MATERIALS AND METHODS

2.1 | Animals

All mice were on the same genetic background (C57BL/6J), group housed without enrichment structures in a specific pathogen-free environment in ventilated cages, and used in the experiments according to the Guideline for the Care and Use of Laboratory Animals of our research facilities. $App^{NL\text{-}F/wt}$ knock-in; *ob/ob* mice were produced by cross-breeding $App^{NL\text{-}F/wt}$ knock-in mice[22] and *ob/ob* mice (Charles River Laboratory Japan, to which B6.Cg-Lep^{ob}/J was introduced from the Jackson Laboratory). Male heterozygous $App^{NL\text{-}F/wt}$ knock-in mice were cross-bred with female heterozygous *ob/+* mice to generate $App^{NL\text{-}F/wt}$ knock-in; *ob/+* founder mice. These male $App^{NL\text{-}F/wt}$ knock-in; *ob/+* founder mice were then cross-bred with female heterozygous *ob/+* mice to obtain $App^{NL\text{-}F/wt}$ knock-in; *ob/ob*, $App^{NL\text{-}F/wt}$ knock-in, *ob/ob*, and WT littermate mice, and housed in in the same cage. We employed two animal cohorts: the young cohort and the old cohort. In the old cohort (n = 169), we recorded date of death from the time when genotypes were determined (~1 month of age), until 18 months of age, when the animals were euthanized for biochemical/histochemical analyses. Notably, 23.7% (40/169) of mice died naturally, while 76.3% (129/169) of mice were euthanized at 18 months. These naturally dead mice were treated as the event, while euthanized mice were censored in the survival analysis. The young cohort (n = 50) was euthanized at 6 months of age for biochemical/histochemical analyses.

2.2 | Tissue collection and sample preparation

Mice were anesthetized with xylazine and ketamine (20 and 100 mg/kg, respectively). Blood was collected by the cardiac puncture. After transcardial perfusion with phosphate buffered saline plus a complete protease inhibitor cocktail (Nacalai Tesque), the brain was removed, divided along the sagittal

plane, and the right hemisphere (cortical and hippocampal areas) was stored at −80°C until the biochemical analysis. The left hemisphere was fixed with 4% of paraformaldehyde overnight and embedded in paraffin for the histological analysis. For the biochemical analysis, tissues were pulverized in a prechilled (on dry ice) BioPulverizer (BioSpec) and homogenized with a polytron homogenizer (KINEMATICA) at a ratio of 20 mL/g of wet weight brain tissue in ice-cold RIPA lysis buffer (Millipore) containing 0.1% SDS or diethylamine (DEA) (for Aβ extraction) and complete protease inhibitor cocktail (Roche) on ice. After centrifugation at 100,000 *g* for 1 hour at 4°C, the supernatant was collected and used for the biochemical analyses. The order of sample preparation and following analyses were randomly assigned independent of genotypes.

2.3 | ELISAs and other biochemical assays

Levels of post-synaptic density 95 (PSD95), glial fibrillary acidic protein (GFAP), and CD11b were determined using ELISAs as previously described.[23] Levels of Aβ x-42 were determined using an ELISA employing a mouse monoclonal BC05 (recognizes C-terminus of Aβ42 [43]) capture antibody and a biotin-conjugated mouse monoclonal BNT77 (recognizes 11-28 aa of Aβ) detection antibody (Wako). A synthetic Aβ 1-42 peptide (Peptide Institute Inc) was used as a standard. Levels of neurofilament heavy chain (NF-H) were determined with an ELISA using a mouse monoclonal SMI 35 capture antibody (BioLegend) and a rabbit polyclonal NF200 detection antibody (Sigma). Purified bovine NF-H (PROGEN) was used as a standard. Levels of synaptotagmin 1 (SYT1) were determined with an ELISA using a rabbit polyclonal SYT1 cytoplasmic tail capture antibody and a biotin-conjugated mouse monoclonal 41.1 detection antibody (Synaptic Systems). Recombinant human SYT1 proteins (Origene) were used as standards. Levels of phospho-tau were determined with an ELISA using a mouse monoclonal Tau5 capture antibody (BioLegend) and a biotin-conjugated mouse AT270 detection antibody (Thermo Fisher Scientific). Synthetic peptides containing both epitopes of Tau5 and AT270 (GenScript) were used as standards. Colorimetric quantification was performed using an iMark plate reader (Bio-Rad) after incubations with horseradish peroxidase (HRP)-linked Avidin-D (Vector) or anti-rabbit IgG (H + L), HRP conjugate (Promega), and the 3,3′,5,5′-tetramethylbenzidine substrate (Sigma). Levels of Aβ x-40 were determined using Human/Rat Aβ (40) ELISA Kit *Wako* II according to the manufacture's protocol (Wako). Levels of insulin were determined using Ultra Sensitive Mouse Insulin ELISA kit according to the manufacture's protocol (Morinaga). Levels of glucose was determined using Glucose Assay Kit-WST according to the manufacture's protocol (Dojindo).

2.4 | Quantitative real-time PCR

Total RNA was purified using RNeasy Lipid Tissue Mini kit (QIAGEN), eluted in nuclease-free water and stored at −80°C. Reverse transcription was performed using ReverTra Ace qPCR RT Master Mix (TOYOBO). Real-time PCR was conducted with the Luna Universal qPCR Master Mix (NEW ENGLAND BioLabs) using an i1000 thermal cycler (Bio-Rad) to detect levels of the TREM2, DAP12, IRS (insulin receptor substrate)-1, IRS-2, PDK1 (pyruvate dehydrogenase kinase 1), INSR (insulin receptor), and β-actin mRNAs. The following primers were used: IRS-1 forward primer CGATGGCTTCTCAGACGTG and reverse primer CAGCCCGCTTGTTGATGTTG; IRS-2 forward primer CTGCGTCCTCTCCCAAAGTG and reverse primer GGGGTCATGGGCATGTAGC; Pdk1 forward primer GGACTTCGGGTCAGTGAATGC and reverse primer TCCTGAGAAGATTGTCGGGGA; INSR forward primer ATGGGCTTCGGGAGAGGAT and reverse primer GGATGTCCATACCAGGGCAC; β-actin forward primer AGTGTGACGTTGACATCCGTA and reverse primer GCCAGAGCAGTAATCTCCTTC; TREM2 forward primer TGCTGGCAAAGGAAAGGT and reverse primer GTTGAGGGCTTGGGACAGG; and DAP12 forward primer GTTGACTCTGCTGATTGCCCT and reverse primer CCCTTCCGCTGTCCCTTGA (Integrated DNA Technologies). The relative expression levels were quantified and analyzed using Bio-Rad iCycler iQ software (Bio-Rad). Relative mRNA levels were calculated using ΔΔCt method with β-actin serving as an internal control for each specific gene amplification reaction.

2.5 | Immunohistochemical staining

Mouse brains were fixed as described above in the section listing the tissue collection and sample preparation methods. Brain samples were embedded in paraffin wax and cut into sections with a thickness of 10 μm. Mouse samples used for immunohistochemical staining were chosen if their ELISA values were similar to the average value for each group. Brain sections were submerged in EDTA buffer (1 mM, pH 8.0), and autoclaved for antigen retrieval. Sections were immersed in 95% of formic acid for Aβ staining. Endogenous peroxidase activity was quenched by incubating the sections with hydrogen peroxide. Sections were incubated with primary antibodies at 4°C overnight. We used an anti-Aβ (6E10, epitope: 3-8 aa of Aβ) antibody (Merck), anti-GFAP antibody (Agilent Technologies), and anti-Iba1 antibody (Wako). Sections were incubated with an HRP-conjugated secondary antibody and diaminobenzidine reaction mixture (Vector Laboratories). Stained sections were observed under a microscope (BZ-X810, Keyence).

2.6 | Statistical analysis

All statistical analyses were performed using JMP Pro software (version 12, SAS Institute Inc). In the survival analysis, Cox proportional hazard models with sex and genotype were as covariates, the date of birth as the time of origin, and the age at death as the time of the event were employed to address the risk of death. In other analyses, effects of each genotype were addressed through (a) the linear regression models adjusting for sex followed by Tukey's HSD test when both genders were included, or (b) one-way ANOVA followed by Tukey's HSD test when one gender was included. *P*-values less than 0.05 were considered significant. Data are presented as adjusted means ± standard errors of the means when both genders were included or means ± standard deviations of the means when one gender was included.

3 | RESULTS

3.1 | The shortest lifespan is observed for *App*$^{NL\text{-}F/wt}$ knock-in; *ob/ob* mice, despite the minimal and comparable increase in Aβ42 levels

We previously crossed amyloid precursor protein (APP) 23 mice with *ob/ob* mice to study the interaction between obesity/diabetes and AD,[9] while a new generation of AD mouse models that express APP at comparable levels to controls has been developed.[22] Thus, we crossed these *App*$^{NL\text{-}F/wt}$ knock-in mice, instead of APP23 mice, with ob/ob to study the interaction between obesity/diabetes and AD. Interestingly, *App*$^{NL\text{-}F/wt}$ knock-in; *ob/ob* mice displayed the shortest lifespan compared to wild-type mice, *App*$^{NL\text{-}F/wt}$ knock-in mice, and *ob/ob* mice (Figure 1A), as supported by the results from the proportional hazard model adjusted for sex (Figure 1B). Such trends were also observed in the analyses stratified by sex (Figure S1). Additionally, *ob/ob* mice had a shorter lifespan than control mice, consistent with a previous study.[24] Lower body weights were recorded for *App*$^{NL\text{-}F/wt}$ knock-in; *ob/ob* mice than *ob/ob* mice after adjusting for sex (Figure 1C), while such trends were significant in only female mice in the analysis stratified by sex (Figure S1). Sex difference is becoming focused in AD research field.[25,26] A new cohort with increased samples will help us to understand the effects of sex on outcomes. We could not measure blood glucose levels during the course of our study until 18 months of age, because any stressful or invasive procedure might have impacts on lifespan of our mice. We measured insulin levels and casual glucose levels in serum from the mice when they were killed at 18 months of age and found that the levels of insulin in *ob/ob* mice and *App*$^{NL\text{-}F/wt}$ knock-in; *ob/ob* mice were comparable and higher than wild-type mice and *App*$^{NL\text{-}F/wt}$ knock-in mice and that there were no significant difference between the groups in casual blood glucose levels (Figure S2).

β-amyloid accumulation in the brains of 18-month-old *App*$^{NL\text{-}F/wt}$ knock-in mice and *App*$^{NL\text{-}F/wt}$ knock-in; *ob/ob* mice was below the detection limit of IHC staining (Figure 2A), consistent with the observation that *App*$^{NL\text{-}F/wt}$ knock-in mice do not form senile plaques until a very old age exceeding 24 months.[22] GuHCl extraction, which requires a greater dilution of samples, did not produce detectable Aβ levels in *App*$^{NL\text{-}F/wt}$ knock-in mice (data not shown). DEA extraction allows us to measure lower Aβ levels using an ELISA.[27] Using DEA extraction, we observed increases in Aβ42 levels in the brains of *App*$^{NL\text{-}F/wt}$

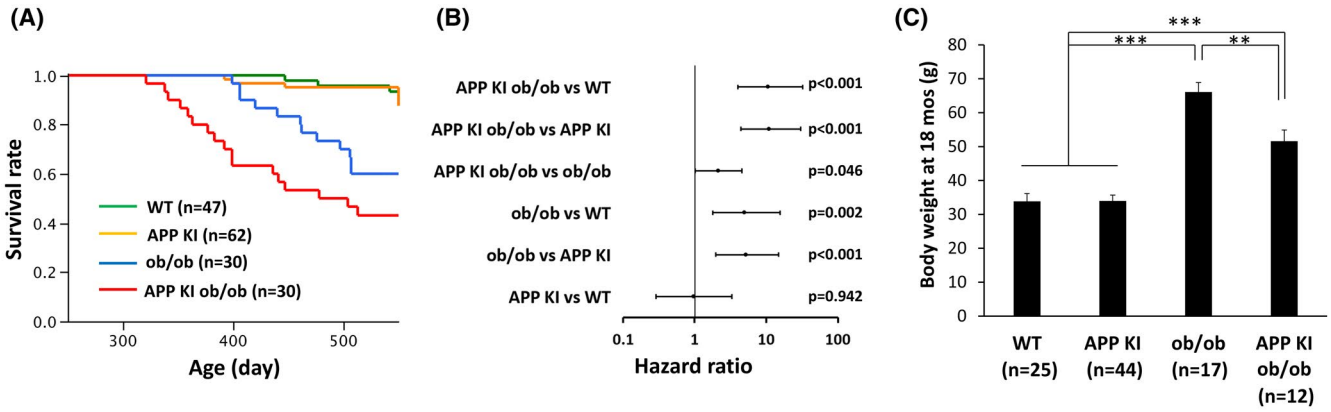

FIGURE 1 Reduced lifespan of *App*$^{NL\text{-}F/wt}$ knock-in; *ob/ob* mice. A, Survival curves for animal cohorts stratified by genotype (n = 30-62 mice/group). B, The hazard ratios, 95% CIs and *P*-values of each genotype were determined using the Cox proportional model after adjusting for sex. C, Body weight was compared among 18-month-old WT, *App*$^{NL\text{-}F/wt}$ knock-in, ob/ob, and *App*$^{NL\text{-}F/wt}$ knock-in; *ob/ob* after adjusting for sex (n = 12-44 mice/group). Data are presented as adjusted means ± standard errors of the means. $^{**}P < .01$, and $^{***}P < .001$ for the comparisons among each genotype using Tukey's HSD test. APP KI, *App*$^{NL\text{-}F/wt}$ knock-in; APP KI ob/ob, *App*$^{NL\text{-}F/wt}$ knock-in; *ob/ob* mice; WT, wild type

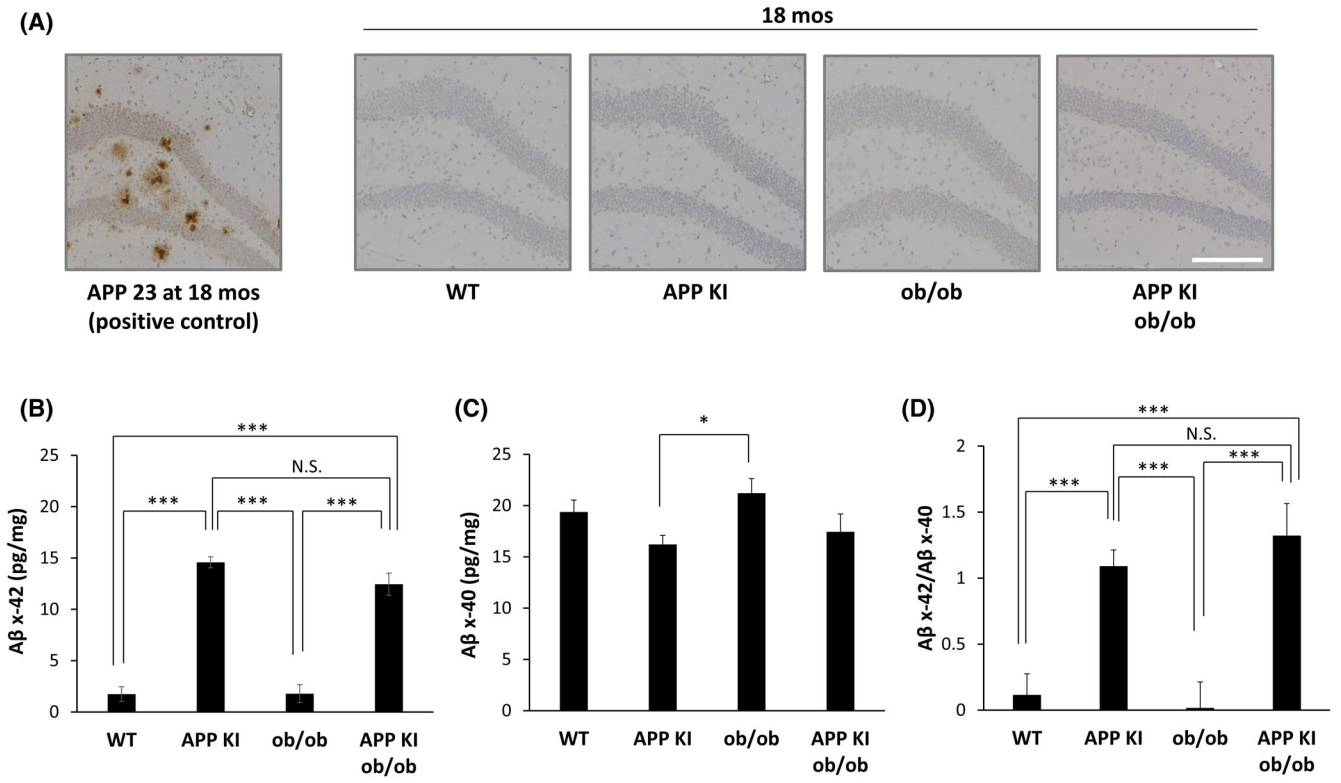

FIGURE 2 Minimal and comparable increases in brain Aβ levels were observed in 18-month-old $App^{NL\text{-}F/wt}$ knock-in; *ob/ob* mice. A, Images of immunohistochemical staining showing no-detectable Aβ accumulation in 18-month-old WT, $App^{NL\text{-}F/wt}$ knock-in, ob/ob, and $App^{NL\text{-}F/wt}$ knock-in; *ob/ob* mice, using APP23 mice at the same age as a positive control (scale bar = 200 μm). Levels of Aβ x-42 (B), Aβ x-40 (C), and ratio of Aβ x-42 to Aβ x-40 (D) in diethylamine-extractable fraction of brains of 18-month-old WT, $App^{NL\text{-}F/wt}$ knock-in, ob/ob, and $App^{NL\text{-}F/wt}$ knock-in; *ob/ob* mice were assessed using an ELISA and compared among each genotype after adjusting for sex (n = 11-44 mice/group). Data are presented as adjusted means ± standard errors of the means. $*P < .05$, and $***P < .001$ for the comparison among each genotype groups using Tukey's HSD test. APP KI, $App^{NL\text{-}F/wt}$ knock-in; APP KI ob/ob, $App^{NL\text{-}F/wt}$ knock-in; *ob/ob* mice; NS , not significant; WT, wild type

knock-in mice or $App^{NL\text{-}F/wt}$ knock-in; *ob/ob* mice, compared to wild-type or *ob/ob* mice (Figure 2B). Their levels were mostly comparable between $App^{NL\text{-}F/wt}$ knock-in mice and $App^{NL\text{-}F/wt}$ knock-in; *ob/ob* mice (Figure 2B), while $App^{NL\text{-}F/wt}$ knock-in; *ob/ob* mice showed some reduction of Aβ42 levels in male group, but not female group (Figure S2). There is no difference or some trends of reduction of Aβ40 levels in the brains of $App^{NL\text{-}F/wt}$ knock-in mice or $App^{NL\text{-}F/wt}$ knock-in; *ob/ob* mice, compared to wild-type or *ob/ob* mice, especially in male group (Figures 2C and S3). However, there is significant increase in the ratio of Aβ42 to Aβ40 by $App^{NL\text{-}F/wt}$ knock-in (Figure 2D), consistent with the previous study.[22]

3.2 | Microglia and astrocytes are dysregulated in $App^{NL\text{-}F/wt}$ knock-in; *ob/ob* mice

To explore the mechanism by which the lifespan of $App^{NL\text{-}F/wt}$ knock-in; *ob/ob* mice are decreased, we initially analyzed the brain levels of neuronal markers, NF-H (Figure 3A), SYT1 (Figure 3B), PSD95 (Figure 3C), and phospho-tau (Figure 3D) through ELISAs, where sample values were in the non-saturable range of standard curve (Figure 3E-H), but did not detect any changes in $App^{NL\text{-}F/wt}$ knock-in mice, *ob/ob* mice, and $App^{NL\text{-}F/wt}$ knock-in; *ob/ob* mice compared to wild-type mice. Because insulin signalling in the brain is involved in regulating the lifespan,[28,29] we also assessed the levels of molecules related to insulin signalling. *Irs2* and *Pdk1* expression were significantly reduced in *ob/ob* mice, but not $App^{NL\text{-}F/wt}$ knock-in; *ob/ob* mice, compared to WT controls (Figure S4). Thus, the shortest lifespan observed in $App^{NL\text{-}F/wt}$ knock-in; *ob/ob* mice may not be explained by a reduction in the expression of molecules involved in neuronal markers or insulin signalling in the brain.

However, the protein expression of a microglial marker, CD11b, was reduced in both *ob/ob* and $App^{NL\text{-}F/wt}$ knock-in; *ob/ob* mice (Figure 4A). Interestingly, mRNA levels of *Trem2* and *Dap12*, genes that are abundantly expressed in microglia and play important roles in AD pathogenesis,[30] were also reduced in both *ob/ob* and $App^{NL\text{-}F/wt}$ knock-in; *ob/ob* mice (Figure 4B,C), while the numbers of Iba1-expressing

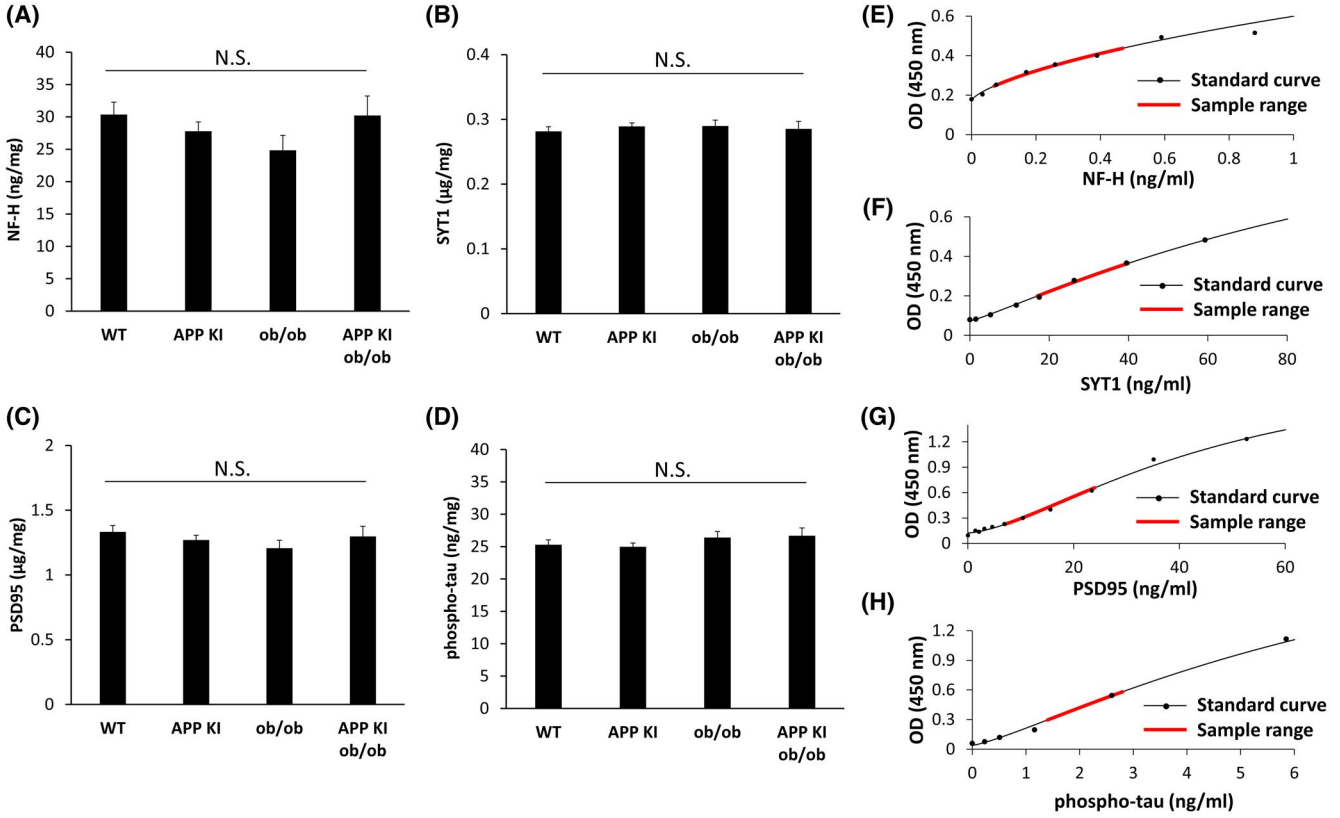

FIGURE 3 Levels of neuronal markers were not altered in 18-month-old *App*$^{NL\text{-}F/wt}$ knock-in; *ob/ob* mice. Levels of NF-H (A), SYT1 (B), PSD95 (C), and phospho-tau (D) were assessed using ELISAs and compared among each genotype after adjusting for sex (n = 10-44 mice/group). Standard curve of ELISAs of NF-H (E), SYT1 (F), PSD95 (G), and phospho-tau (H) with sample range as shown in red line in a representative assay. A-D, Data are presented as adjusted means ± standard errors of the means and were compared among each genotype using Tukey's HSD test. APP KI, *App*$^{NL\text{-}F/wt}$ knock-in; APP KI ob/ob, *App*$^{NL\text{-}F/wt}$ knock-in; *ob/ob* mice; NS, not significant; WT, wild type

microglia assessed by IHC staining were not altered (Figure S5). Moreover, levels of the astrocytic marker GFAP were increased in *App*$^{NL\text{-}F/wt}$ knock-in; *ob/ob* mice, compared to *ob/ob* mice, as determined using an ELISA and IHC staining (Figure 4D,E).

We also analyzed young mice that were harvested at 6 months old. Notably, body weights were comparable between *ob/ob* mice and *App*$^{NL\text{-}F/wt}$ knock-in; *ob/ob* mice at this age (Figure 5A), suggesting that decrease of body weight at 18 months old occurred after this age. The levels of synaptic markers (SYT1 and PSD95), but not NF-H, were increased in young *App*$^{NL\text{-}F/wt}$ knock-in; *ob/ob* mice compared to wild-type mice (Figure 5B-D). To investigate the mechanisms of upregulation of the protein levels of SYT1 and PSD95, we performed quantitative real-time PCR for these molecules. Expressions of *Syt1* and *Psd95* tended to increase, but not significantly, in young *App*$^{NL\text{-}F/wt}$ knock-in; *ob/ob* mice (Figure S6). These data might suggest that biological mechanisms such as compensation, homeostasis, or some response to Aβ and metabolic changes might function at transcriptional levels in *App*$^{NL\text{-}F/wt}$ knock-in; *ob/ob* mice at an early age, although further studies are needed. Moreover, at a young age, GFAP levels were decreased in *App*$^{NL\text{-}F/wt}$ knock-in; *ob/ob* mice, while CD11b levels showed the same trends as in older mice (Figure 5E,F). Thus, among several molecules assessed, including Aβ, tau, synaptic or neuronal markers, insulin signalling markers, and neuroinflammatory cell markers, only the levels of markers of microglia and astrocytes were specifically altered in *App*$^{NL\text{-}F/wt}$ knock-in; *ob/ob* mice in an age-dependent manner, suggesting potential roles for microglia and astrocytes in decreasing the lifespan of the AD model mice with diabetes.

4 | DISCUSSION

While clinical studies have indicated associations between obesity/diabetes and AD and neurodegeneration, it has been not clearly determined whether these diseases interact with each other to alter lifespan. As shown in the present study using *App*$^{NL\text{-}F/wt}$ knock-in; *ob/ob* mice obtained by crossing *App*$^{NL\text{-}F/wt}$ knock-in mice and *ob/ob* mice, increased Aβ42 levels affected the lifespan of *ob/ob* mice through a

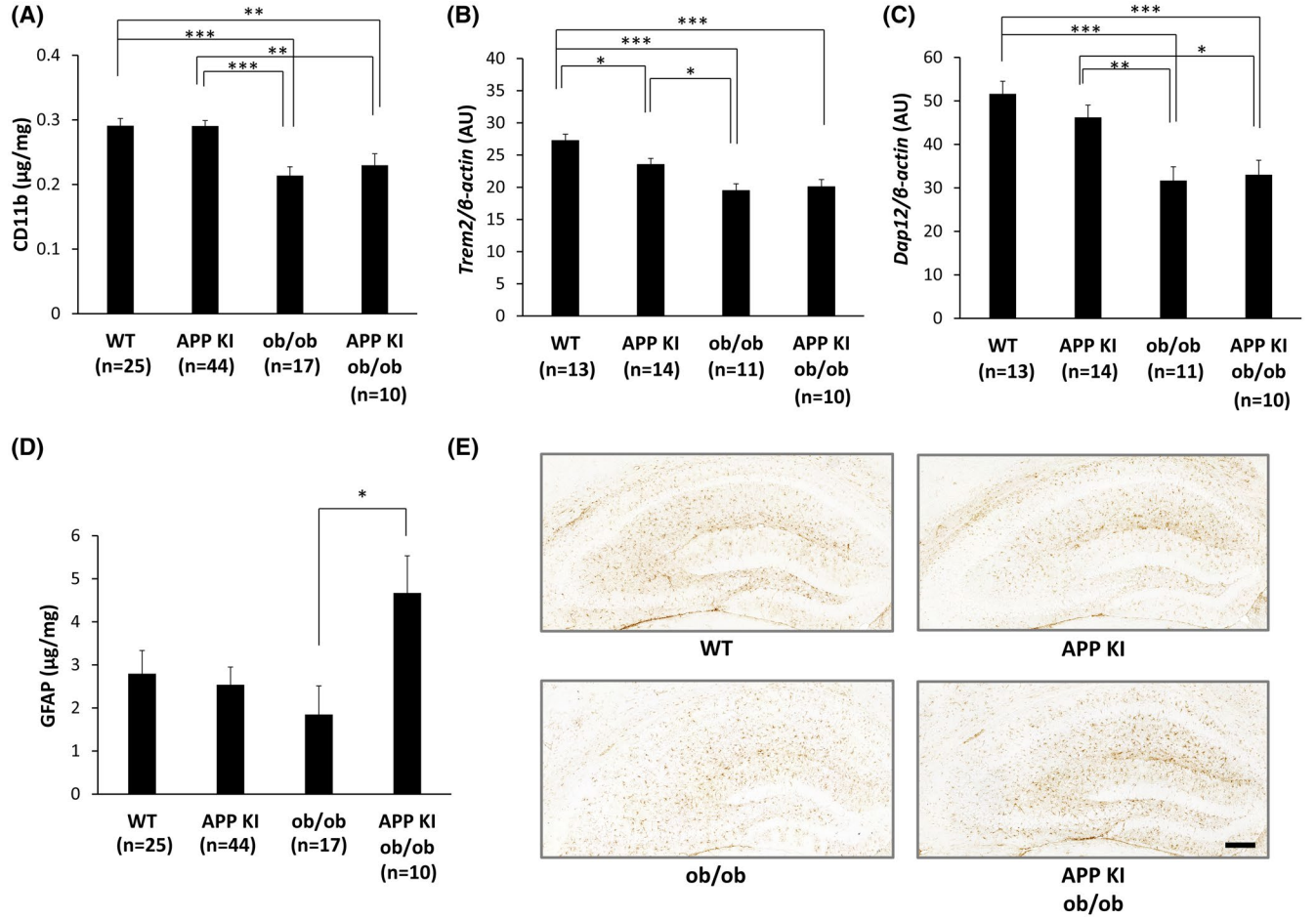

FIGURE 4 Dysregulation of microglia and astrocytes in 18-month-old $App^{NL\text{-}F/wt}$ knock-in; *ob/ob* mice. Levels of CD11b (A) and GFAP (D) were assessed using ELISAs and compared among each genotype after adjusting for sex (n = 10-44 mice/group). Levels of the TREM2 (B) and DAP12 (C) mRNAs were assessed using real-time PCR and compared among each genotype after adjusting for sex (n = 10-14 mice/group). Images of immunohistochemical staining for GFAP in WT, $App^{NL\text{-}F/wt}$ knock-in, *ob/ob*, and $App^{NL\text{-}F/wt}$ knock-in; *ob/ob* mice (scale bar = 200 μm) (E). Data are presented as adjusted means ± standard errors of the means. $^{*}P < .05$, $^{**}P < .01$, and $^{***}P < .001$ for the comparisons among each genotype using Tukey's HSD test. APP KI, $App^{NL\text{-}F/wt}$ knock-in; APP KI ob/ob, $App^{NL\text{-}F/wt}$ knock-in; *ob/ob* mice; WT, wild type

mechanism associated with the dysregulation of microglia and astrocytes.

Both dementia and obesity/diabetes are associated with a shorter life expectancy.[5,6,8] In the present study, $App^{NL\text{-}F/wt}$ knock-in; *ob/ob* mice had the shortest lifespan compared to wild-type mice, $App^{NL\text{-}F/wt}$ knock-in mice, and *ob/ob* mice. Additionally, *ob/ob* mice had a shorter lifespan than control mice, consistent with a previous reported.[24] Patients with both Apoε4 and diabetes have a shorter lifespan than individuals with Apoε4 and without diabetes, individuals without Apoε4 and with diabetes, and subjects with neither Apoε4 nor diabetes (Shinohara and Sato, *unpublished results*). Because Apoε4 is a strong genetic risk factor for AD, the results of the present study using an animal model of AD indicate a possible interaction between obesity/diabetes and AD on altering the lifespan of humans. Further human studies are required to confirm this observation.

There is a significant weight loss in $App^{NL\text{-}F/wt}$ knock-in; *ob/ob* mice compared to *ob/ob* mice, especially in female mice at old age. Because food intake and/or energy expenditure are reported to be altered in some AD models,[31,32] measurement of these parameters would be interesting. Frailty is also associated with AD.[33] If this weight loss is linked to frailty, the weight loss may also impact survival. Further studies including food intake, energy expenditure, and frailty index are required to determine the mechanisms of weight loss in $App^{NL\text{-}F/wt}$ knock-in; *ob/ob* mice.

In the present study, comparable Aβ levels were observed between $App^{NL\text{-}F/wt}$ knock-in mice and $App^{NL\text{-}F/wt}$ knock-in; *ob/ob* mice. Firm evidence showing that diabetes increases Aβ deposition in humans is not currently available,[34,35] although diabetes/hyperglycaemia modify Aβ accumulation in the brains of wild-type animals[36] and animal models of AD.[9,37,38] Moreover, several neuropathological studies

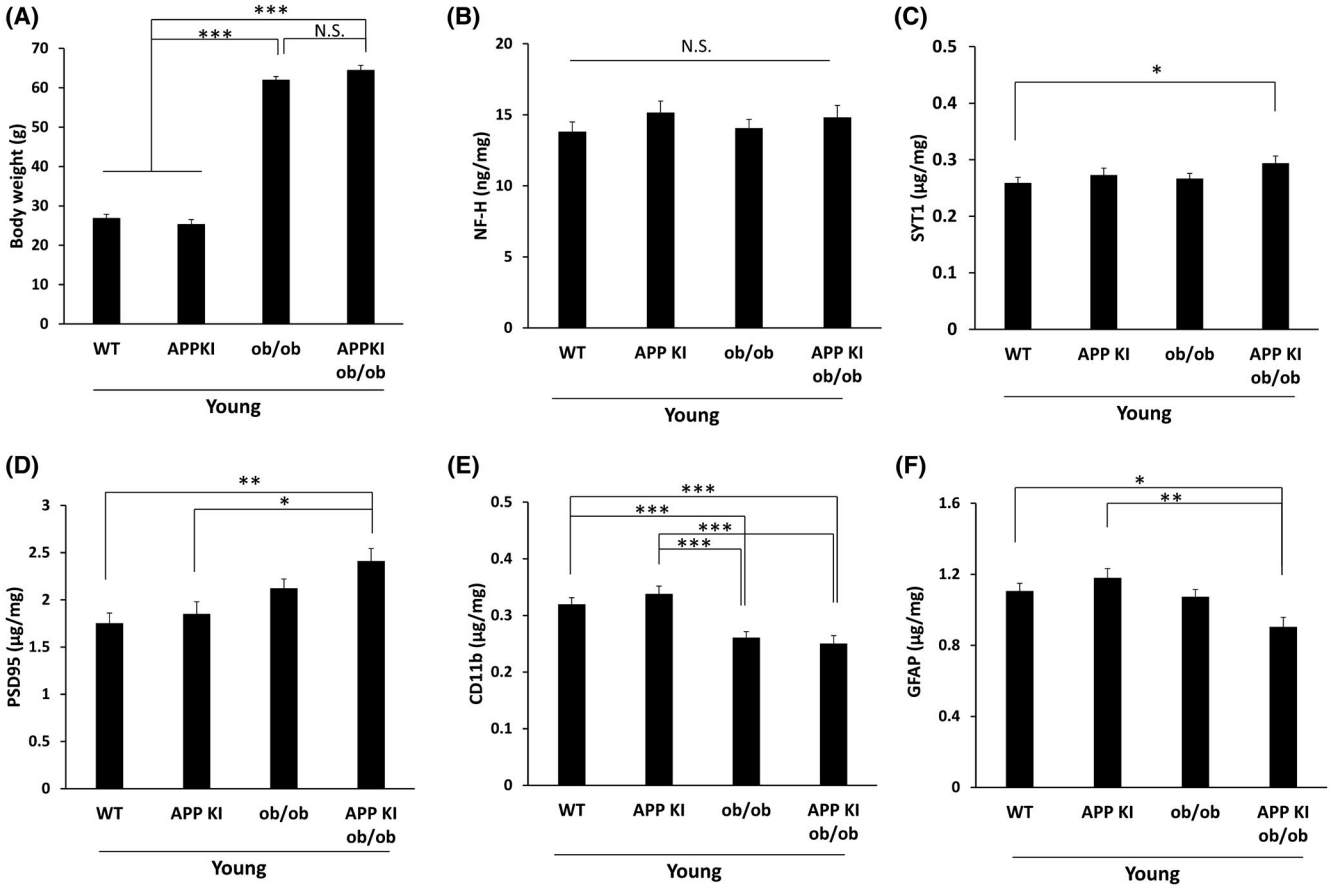

FIGURE 5 Levels of neuronal and glial markers in young (6-month-old) $App^{NL\text{-}F/wt}$ knock-in; *ob/ob* mice. A, Body weight of young mice were compared among each genotype after adjusting for sex (n = 8-17 mice/group). B-F, Levels of NF-H (B), SYT1 (C), PSD95 (D), CD11b (E), and GFAP (F) in the brains of young mice were compared among each genotype after adjusting for sex (n = 9-17 mice/group). Data are presented as adjusted means ± standard errors of the means. $*P < .05$, $**P < .01$, and $***P < .001$ for the comparisons among each genotype using Tukey's HSD test. APP KI, $App^{NL\text{-}F/wt}$ knock-in; APP KI ob/ob, $App^{NL\text{-}F/wt}$ knock-in; *ob/ob* mice; NS, not significant; WT, wild type

revealed less senile plaques in patients with AD who have been diagnosed with diabetes compared with patients without diabetes.[13] Thus, we may be able to consider the observation that obesity/diabetes and AD interact to determine lifespan when attempting to obtain a better understanding of the discrepancies among the results of neuropathological studies.

Obesity and diabetes are associated with the dysregulation of macrophages in the peripheral system in humans and animal models.[39-41] Indeed, Obesity and diabetes increase the susceptibility to infection and impairs wound healing.[39,42-44] Recently, emerging evidence supports the hypothesis that the dysfunction of microglia, the counterpart of macrophages in the brain, plays important roles in the pathogenesis of AD.[45-47] In the present study, levels of the microglial marker CD11b were reduced in *ob/ob* and $App^{NL\text{-}F/wt}$ knock-in; *ob/ob* mice at both 6 and 18 months. Interestingly, the expression of *Trem2* and its partner *Dap12* were also reduced in these mice. Based on accumulating evidence from recent studies, a reduction in the activity of the TREM2 signalling pathway promotes neurodegeneration.[30,48] Because brain Aβ42 levels were comparable in $App^{NL\text{-}F/wt}$ knock-in mice and $App^{NL\text{-}F/wt}$ knock-in; *ob/ob* mice, soluble Aβ42 might not be targeted by microglia. Rather, the dysregulation of microglia may cause susceptibility to Aβ.

We observed increased GFAP levels in 18-month-old $App^{NL\text{-}F/wt}$ knock-in; *ob/ob* mice, while its levels decreased in 6-month-old animals. Their age-dependent increases were also observed immunohistochemically (Figure S7). Thus, astrocytes might be activated by obesity/diabetes and AD during aging. The activated astrocytes may be reactive astrocytes. Recent studies indicate that reactive astrocytes obtain neurotoxic properties both through a gain of toxic function and a loss of their neurotrophic effects and affect AD pathogenesis, although astrocyte reactions might also be heterogeneous.[49] Because the level of Aβ was not increased in $App^{NL\text{-}F/wt}$ knock-in; *ob/ob* mice compared to $App^{NL\text{-}F/wt}$ knock-in mice, one possible mechanism is that astrocytes might be more vulnerable to the same level of Aβ in $App^{NL\text{-}F/wt}$ knock-in; *ob/ob* mice with dysregulated microglia. Further

studies, including single-cell analyses, would be required to test this hypothesis.

Because insulin signalling in the brain is involved in regulating the lifespan, we assessed the expression of molecules involved in insulin signalling. *Irs2* expression was significantly reduced in *ob/ob* mice, but not $App^{NL\text{-}F/wt}$ knock-in; *ob/ob* mice. Thus, the shortest lifespan observed in $App^{NL\text{-}F/wt}$ knock-in; *ob/ob* mice may not be explained by the decrease in the expression of molecules involved in insulin signalling. The samples analyzed in the present study were obtained from 18-month-old mice that survived to this age. Because, we were unable to analyze the mice that died before reaching 18 months of age, the precise mechanism underlying the substantially decreased lifespan of $App^{NL\text{-}F/wt}$ knock-in; *ob/ob* mice should be analyzed further in future studies.

There are several limitations in our animal models. We chose $App^{NL\text{-}F/wt}$ knock-in mice as an AD model and *ob/ob* mice as a model of obesity linked to diabetes, with affected peripheral insulin signalling (Figure S8), in this study. $App^{NL\text{-}F/wt}$ knock-in mice do not show any amyloid pathology or neurodegenerative changes[22] as shown in this study, and *ob/ob* mice become obese and mildly diabetic due to leptin deficiency.[50,51] In the future study, we will study the interaction between obesity/diabetes and AD on lifespan in both humans and other animal models. In this study as shown in the original report of $App^{NL\text{-}F/wt}$ knock-in mice,[22] there is no difference in lifespan between $App^{NL\text{-}F/wt}$ knock-in mice and wild-type mice until 18 months. Further observational studies to older ages are required to determine whether Aβ42 decrease lifespan in wild-type background, in additions to *ob/ob* background. Alternatively, there is also a possibility that Aβ42 decrease lifespan only in *ob/ob* background, but not in wild-type background, suggesting that Aβ42 is enough toxic to decrease lifespan only in *ob/ob* background, but not in wild-type background. It would be also interesting to see the results of the investigation of $App^{NL\text{-}F/wt}$ knock-in; *ob/ob* mice at 24 months of age when $App^{NL\text{-}F/wt}$ knock-in mice show the formation of senile plaques in the brain. However, we terminated this study at 18 months of age to analyze the mechanism of the shorter lifespan in $App^{NL\text{-}F/wt}$ knock-in; *ob/ob* mice using the tissues of mice which survived until 18 months of age. Further investigation, including the analysis of $App^{NL\text{-}F/NL\text{-}F}$ knock-in mice with senile plaques, will allow us to investigate the impact of senile plaque formation on lifespan in *ob/ob* mice.

In summary, increased levels of Aβ42 decreased the lifespan of *ob/ob* mice and were associated with the dysregulation of microglia and astrocytes. These findings may provide evidence of an interaction between obesity/diabetes and AD to regulate the lifespan. An understanding of the precise mechanisms of this interaction will likely provide novel targets for the treatment of obesity/diabetes and AD.

5 | CONCLUSIONS

The increased Aβ42 levels may decrease the lifespan of *ob/ob* mice, which is associated with the dysregulation of microglia and astrocytes. The imbalance in these neuroinflammatory cells may provide a clue to the mechanisms by which the interaction between obesity/diabetes and early AD reduces life expectancy.

ACKNOWLEDGMENTS

We would like to thank Ms Tomomi Tajiri for providing technical assistance, Dr Noboru Ogiso for providing technical support in the Laboratory of Experimental Animals at National Center for Geriatrics and Gerontology (NCGG) and Dr Wataru Ohashi for discussion on statistics. We also thank lab members in the Department of Aging Neurobiology at NCGG and Dr Masashi Narita for participating in helpful discussions.

DISCLOSURE STATEMENT

The authors have no conflicts of interest related to the content of this article to declare.

AUTHOR CONTRIBUTIONS

N. Sato and Mi. Shinohara designed research; Mi. Shinohara, Y. Tashiro, Mo. Shinohara, J. Hirokawa, M. Onishi-Takeya, and M. Mukouzono performed research; K. Suzuki, S. Takeda, A. Fukumori, and R. Morishita analyzed data; N. Sato and Mi. Shinohara wrote the paper; T. Saito and T.C. Saido contributed to providing a new AD model mouse.

REFERENCES

1. Sato N, Morishita R. Brain alterations and clinical symptoms of dementia in diabetes: abeta/tau-dependent and independent mechanisms. *Front Endocrinol (Lausanne)*. 2014;5:143.
2. Kivipelto M, Ngandu T, Fratiglioni L, et al. Obesity and vascular risk factors at midlife and the risk of dementia and Alzheimer disease. *Arch Neurol*. 2005;62:1556-1560.
3. Shinohara M, Sato N. Bidirectional interactions between diabetes and Alzheimer's disease. *Neurochem Int*. 2017;108:296-302.
4. Sutherland GT, Lim J, Srikanth V, Bruce DG. Epidemiological approaches to understanding the link between type 2 diabetes and dementia. *J Alzheimers Dis*. 2017;59:393-403.
5. Livingstone SJ, Levin D, Looker HC, et al. Estimated life expectancy in a Scottish cohort with type 1 diabetes, 2008–2010. *JAMA*. 2015;313:37-44.
6. Wright AK, Kontopantelis E, Emsley R, et al. Life expectancy and cause-specific mortality in type 2 diabetes: A population-based cohort study quantifying relationships in ethnic subgroups. *Diabetes Care*. 2017;40:338-345.
7. Peeters A, Barendregt JJ, Willekens F, et al. Obesity in adulthood and its consequences for life expectancy: a life-table analysis. *Ann Intern Med*. 2003;138:24-32.
8. Wolfson C, Wolfson DB, Asgharian M, et al. A reevaluation of the duration of survival after the onset of dementia. *N Engl J Med*. 2001;344:1111-1116.

9. Takeda S, Sato N, Uchio-Yamada K, et al. Diabetes-accelerated memory dysfunction via cerebrovascular inflammation and Abeta deposition in an Alzheimer mouse model with diabetes. *Proc Natl Acad Sci USA*. 2010;107:7036-7041.
10. Sato N, Morishita R. Roles of vascular and metabolic components in cognitive dysfunction of Alzheimer disease: short- and long-term modification by non-genetic risk factors. *Front Aging Neurosci*. 2013;5:64.
11. Takeda S, Sato N, Uchio-Yamada K, et al. Oral glucose loading modulates plasma β-amyloid level in Alzheimer's disease patients: Potential diagnostic method for Alzheimer's disease. *Dement Geriatr Cogn Disord*. 2012;34:25-30.
12. Arvanitakis Z, Schneider JA, Wilson RS, et al. Diabetes is related to cerebral infarction but not to AD pathology in older persons. *Neurology*. 2006;67:1960-1965.
13. Kalaria RN. Neurodegenerative disease: Diabetes, microvascular pathology and Alzheimer disease. *Nat Rev Neurol*. 2009;5:305-306.
14. Talbot K, Wang HY, Kazi H, et al. Demonstrated brain insulin resistance in Alzheimer's disease patients is associated with IGF-1 resistance, IRS-1 dysregulation, and cognitive decline. *J Clin Invest*. 2012;122:1316-1338.
15. Starks EJ, O'Grady JP, Hoscheidt SM, et al. Insulin resistance is associated with higher cerebrospinal fluid tau levels in asymptomatic APOE epsilon4 carriers. *J Alzheimers Dis*. 2015, 46(2), 525-533.
16. Vemuri P, Knopman DS, Lesnick TG, et al. Evaluation of amyloid protective factors and Alzheimer disease neurodegeneration protective factors in elderly individuals. *JAMA Neurol*. 2017;74:718-726.
17. Sato N, Morishita R. Plasma abeta: a possible missing link between Alzheimer disease and diabetes. *Diabetes*. 2013;62:1005-1006.
18. Hiller AJ, Ishii M. Disorders of body weight, sleep and circadian rhythm as manifestations of hypothalamic dysfunction in Alzheimer's disease. *Frontiers in Cellular Neuroscience*. 2018;12.
19. Clarke JR, Lyra e Silva NM, Figueiredo CP, et al. Alzheimer-associated Aβ oligomers impact the central nervous system to induce peripheral metabolic deregulation. *EMBO Mol Med*. 2015;7:190-210.
20. Gotaro K, Ann L, Steve I, Kate W. Prevalence of frailty in mild to moderate Alzheimer's disease: A systematic review and meta-analysis. *Curr Alzheimer Res*. 2017;14:1256-1263.
21. Zhang Y, Zhou B, Zhang F, et al. Amyloid-β induces hepatic insulin resistance by activating JAK2/STAT3/SOCS-1 signaling pathway. *Diabetes*. 2012;61:1434-1443.
22. Saito T, Matsuba Y, Mihira N, et al. Single App knock-in mouse models of Alzheimer's disease. *Nat Neurosci*. 2014;17:661-663.
23. Shinohara M, Fujioka S, Murray ME, et al. Regional distribution of synaptic markers and APP correlate with distinct clinicopathological features in sporadic and familial Alzheimer's disease. *Brain*. 2014;137:1533-1549.
24. Austin BP, Garthwaite TL, Hagen TC, Stevens JO, Menahan LA. Hormonal, metabolic and morphologic studies of aged C57BL/6J obese mice. *Exp Gerontol*. 1984;19:121-132.
25. Buckley RF, Mormino EC, Chhatwal J, et al. Associations between baseline amyloid, sex, and APOE on subsequent tau accumulation in cerebrospinal fluid. *Neurobiol Aging*. 2019;78:178-185.
26. Oveisgharan S, Arvanitakis Z, Yu L, Farfel J, Schneider JA, Bennett DA. Sex differences in Alzheimer's disease and common neuropathologies of aging. *Acta Neuropathol*. 2018;136:887-900.
27. Shinohara M, Sato N, Kurinami H, et al. Reduction of brain β-amyloid (Aβ) by fluvastatin, a hydroxymethylglutaryl-CoA reductase inhibitor, through increase in degradation of amyloid precursor protein C-terminal fragments (APP-CTFs) and Aβ clearance. *J Biol Chem*. 2010;285:22091-22102.
28. Akintola AA, van Heemst D. Insulin, aging, and the brain: mechanisms and implications. *Front Endocrinol*. 2015;6:13-13.
29. Taguchi A, Wartschow LM, White MF. Brain IRS2 signaling coordinates life span and nutrient homeostasis. *Science*. 2007;317:369-372.
30. Ulland TK, Colonna M. TREM2—a key player in microglial biology and Alzheimer disease. *Nat Rev Neurol*. 2018;14:667-675.
31. Vloeberghs E, Van Dam D, Franck F, et al. Altered ingestive behavior, weight changes, and intact olfactory sense in an APP overexpression model. *Behav Neurosci*. 2008;122:491-497.
32. Adebakin A, Bradley J, Gumusgoz S, Waters EJ, Lawrence CB. Impaired satiation and increased feeding behaviour in the triple-transgenic Alzheimer's disease mouse model. *PLoS ONE*. 2012;7:e45179.
33. Wallace LMK, Theou O, Godin J, Andrew MK, Bennett DA, Rockwood K. Investigation of frailty as a moderator of the relationship between neuropathology and dementia in Alzheimer's disease: a cross-sectional analysis of data from the Rush Memory and Aging Project. *Lancet Neurol*. 2019;18:177-184.
34. Roberts RO, Knopman DS, Cha RH, et al. Diabetes and elevated hemoglobin a1c levels are associated with brain hypometabolism but not amyloid accumulation. *J Nucl Med*. 2014;55:759-764.
35. Tomita N, Furukawa K, Okamura N, et al. Brain accumulation of amyloid beta protein visualized by positron emission tomography and BF-227 in Alzheimer's disease patients with or without diabetes mellitus. *Geriatr Gerontol Int*. 2013;13:215-221.
36. Sparks DL, Scheff SW, Hunsaker JC 3rd, Liu H, Landers T, Gross DR. Induction of Alzheimer-like beta-amyloid immunoreactivity in the brains of rabbits with dietary cholesterol. *Exp Neurol*. 1994;126:88-94.
37. Refolo LM, Malester B, LaFrancois J, et al. Hypercholesterolemia accelerates the Alzheimer's amyloid pathology in a transgenic mouse model. *Neurobiol Dis*. 2000;7:321-331.
38. Ho L, Qin W, Pompl PN, et al. Diet-induced insulin resistance promotes amyloidosis in a transgenic mouse model of Alzheimer's disease. *Faseb J*. 2004;18:902-904.
39. Falanga V. Wound healing and its impairment in the diabetic foot. *Lancet*. 2005;366:1736-1743.
40. Shultz LD, Schweitzer PA, Christianson SW, et al. Multiple defects in innate and adaptive immunologic function in NOD/LtSz-scid mice. *J Immunol*. 1995;154:180-191.
41. Castoldi A, Naffah de Souza C, Camara NO, Moraes-Vieira PM. The macrophage switch in obesity development. *Front Immunol*. 2015;6:637.
42. Ratter JM, Tack CJ, Netea MG, Stienstra R. Environmental signals influencing myeloid cell metabolism and function in diabetes. *Trends Endocrinol Metab*. 2018;29(7):468-480.
43. Dinh T, Tecilazich F, Kafanas A, et al. Mechanisms involved in the development and healing of diabetic foot ulceration. *Diabetes*. 2012;61:2937-2947.
44. Pierpont YN, Dinh TP, Salas RE, et al. Obesity and surgical wound healing: a current review. *ISRN Obes*. 2014;2014:638936.
45. Guerreiro R, Wojtas A, Bras J, et al. TREM2 variants in Alzheimer's disease. *N Engl J Med*. 2012;368:117-127.
46. Jonsson T, Stefansson H, Steinberg S, et al. Variant of TREM2 associated with the risk of Alzheimer's disease. *N Engl J Med*. 2012;368:107-116.

47. Hansen DV, Hanson JE, Sheng M. Microglia in Alzheimer's disease. *J Cell Biol*. 2018;217:459.
48. Carmona S, Zahs K, Wu E, Dakin K, Bras J, Guerreiro R. The role of TREM2 in Alzheimer's disease and other neurodegenerative disorders. *Lancet Neurol*. 2018;17:721-730.
49. Perez-Nievas BG, Serrano-Pozo A. Deciphering the astrocyte reaction in Alzheimer's disease. *Front Aging Neurosci*. 2018;10:114.
50. Kleinert M, Clemmensen C, Hofmann SM, et al. Animal models of obesity and diabetes mellitus. *Nat Rev Endocrinol*. 2018;14:140-162.
51. Menahan LA. Age-related changes in lipid and carbohydrate metabolism of the genetically obese mouse. *Metabolism*. 1983;32:172-178.

SUPPORTING INFORMATION

Additional supporting information may be found online in the Supporting Information section.

How to cite this article: Shinohara M, Tashiro Y, Shinohara M, et al. Increased levels of Aβ42 decrease the lifespan of *ob/ob* mice with dysregulation of microglia and astrocytes. *The FASEB Journal*. 2019;00:1–11. https://doi.org/10.1096/fj.201901028RR